HHS Public Access

Author manuscript

Anal Biochem. Author manuscript; available in PMC 2019 December 11.

Published in final edited form as:

Anal Biochem. 1995 November 20; 232(1): 92–97. doi:10.1006/abio.1995.9955.

A Lifetime-Based Fluorescence Resonance Energy Transfer Sensor for Ammonia

Qing Chang[*], **Jeffrey Sipior**[†], **Joseph R. Lakowicz**[†,‡], **Govind Rao**[*,‡,1]

[*]Department of Chemical and Biochemical Engineering, University of Maryland Baltimore County, TRC Building, 5200 Westland Boulevard, Baltimore, Maryland 21227;

[†]Department of Biological Chemistry, Center for Fluorescence Spectroscopy, University of Maryland at Baltimore, 108 North Greene Street, Baltimore, Maryland 21201-1503;

[‡]The Medical Biotechnology Center of the Maryland Biotechnology Institute, University of Maryland at Baltimore, Baltimore, Maryland 20201

Abstract

A lifetime-based optical NH_3 sensor based on the principle of fluorescence resonance energy transfer was developed. The sensor consisted of sulforhodamine 101 as the donor, bromocresol green as the acceptor, ethyl cellulose as the polymer support, and tributyl phosphate as the plasticizer. When the concentration of NH_3 changed, it caused a change in the decay time of the SR101, which was measured by phase-modulation fluorometry. At 100 MHz, increasing the concentration of NH_3 from 0 to 175 ppm resulted in a decrease in phase angle of about 31° and an increase in modulation of about 18%. Oxygen and carbon dioxide did not interfere with the sensor. However, a 30% relative humidity could cause a downward shift of the response by 5°, while additional increase in the relative humidity to 100% showed little further effect. For a film thickness of 40 μm, the typical response and recovery times for 90% of total signal change were 1 and 2.5 min, respectively. The phase angle measurements for the same sample were reproducible for 5 days, with no special care of the film sample.

Optical chemical sensors are of interest in many fields, including biomedical, environmental, and industrial applications (1–3) and bioreactor and bioprocess monitoring (4,5). These sensors utilize either a colorimetric or a fluorometric indicator which is sensitive to the analyte of interest and exhibits a change in absorbance, fluorescence intensity, or fluorescence life time when the concentration of the analyte changes. Sensors based on intensity measurements, e.g., absorbance or fluorescence, are often subject to signal drift resulting from leaching and photobleaching of the indicator dye, variations of light source intensity, and stability of a photodetector. Although wavelength–ratiometric techniques provide a means of overcoming these difficulties, few ratiometric fluorophores are available. Lifetime-based sensing, on the other hand, is independent of fluorophore concentration and variations in the intensity of the light source and is an internally referenced method. Therefore it displays excel lent long-term stability and ease of calibration.

[1]To whom correspondence should be addressed. Fax: (410) 455 6500. grao@umbc.edu.

The lifetime of a fluorophore can be measured by either time-domain or frequency-domain methods (6,7). The frequency-domain method of measuring phase and modulation can provide rapid measurement with simple instrumentation. In this method, a modulated light is used as the excitation light source, which forces the emission light of the fluorophore to also be modulated, but with a lifetime-dependent delay in phase angle and decrease in modulation. For a single exponential decay, the phase angle shift, ϕ, and the demodulation factor, m, are related to the lifetime of the fluorophore by

$$\tan \phi = \omega \tau_{\mathrm{p}} \quad [1]$$

$$m = \left(1 + \omega^2 \tau_{\mathrm{m}}^2\right)^{-1/2} \quad [2]$$

where, $\omega = 2\pi \cdot$(frequency of excitation light), and τ_{p}, the lifetime obtained from the phase angle, is equal to τ_{m}, the lifetime from the demodulation factor. For a multiexponential decay or nonexponential decay, the apparent lifetimes are only interpretations of the measured values of ϕ and m (6) and are no longer equal to each other. The relations between phase angle, demodulation factor and these apparent lifetimes are more complicated. One is referred to Ref. (6) for more details.

The demands for NH_3 sensors come mainly from in dustrial and environmental monitoring of toxic chemicals (8–13) and biotechnology and bioengineering (14,15). Among the optical NH_3 sensors developed so far, the indicator dyes used in absorbance-based sensors include bromophenol blue (8,9,16), bromocresol purple (11,12,16,17), bromocresol green (16), bromothymol blue (18, 19), chlorophenol red (18), *p*-nitrophenol (20), and *p*-xylene blue (16). For fluorescence intensity-based NH_3 sensors, the probes 2-naphthol (8), 5-carboxy-4′, 5′-dimethylfluorescein (14), 2,7-bis(2-car boxyethyl)-5-carboxyfluorescein (14), acridine orange(15), 1-hydroxypyren-3,6,8-trisulfonate (15), and 1- naphthol-4-sulfonate have been employed as the indicators. The laser dye oxazine perchlorate has also been used in an absorbance-based sensor by monitoring the transmission change at 560 nm (13). The performance of these sensors varies. The detection limit of these sensors is generally a few ppm for gaseous NH_3 and μM for aqueous solutions, whereas an exceptionally sensitive one may detect a 7 nM solution of NH_3 (14). Typical response times are in the range of 1 to 60 min. However, a sensor containing bromocresol purple embedded in a porous SiO_2 matrix fabricated using the sol-gel technique possesses a response time of 10 s (17).

All the NH_3 sensors reported so far are based upon either absorbance or fluorescence intensity. Though the instrumentation is simple, in practice intensity-based sensing often suffers from uncontrolled variations in the output signal due to the factors other than the analyte. One such example follows. In the application of an optical sensor in practice, it is frequently required to couple the sensor element with fiber optics. However, bending of the fiber optics causes power attenuation (21), and this can easily alter the output signal to a degree beyond the tolerance of measurement. To pre vent the bending effect, fibers have been fixed on the bench (22). This obviously remains a problem when the sensor is used for field work. Furthermore, as mentioned earlier, the stability of light source intensity and photodetector sensitivity and the leaching and photobleaching of indicator dye are other

difficulties encountered in intensity-based sensing. In contrast, lifetime-based sensing is not subject to these factors, because the decay time of a fluorophore is independent of intensity as long as the signal is detectable.

In this paper, we present the first lifetime-based fluorescence resonance energy transfer (FRET)[2] sensor for NH_3. Recently, it has been demonstrated (23,24) that lifetime-based pH and pCO_2 sensors can be created based on the fluorescence resonance energy transfer principle (6), using phase-modulation fluorometry. In these sensors, a fluorophore serves as the donor and a colorimetric dye which responds to the analyte serves as the acceptor. For efficient energy transfer, the absorption spectrum of the acceptor must overlap with the emission spectrum of the donor. As the concentration of the analyte varies, the absorption spectrum of the acceptor changes. This alters the degree of the overlap and therefore affects the fluorescence intensity and the lifetime of the fluorophore. Another essential requirement for FRET to occur is that the distance between the donor and acceptor must be comparable to the Förster distance. This is generally achieved by adjusting the concentration of the acceptor. A sensor can be based either on a single fluorophore which displays sensitivity to the analyte or on FRET, in which case the fluorophore is insensitive to the analyte and the acceptor is sensitive to the analyte. The use of FRET frequently simplifies identification of a suitable fluorophore because it is difficult to find fluorophores which display both desired spectral properties and sensitivity to the analyte in the desired concentration range.

Like other optical NH_3 sensors, the sensor we report here is based on the pH change induced by the presence of NH_3 in the sensor matrix. The change in pH alters the absorption spectrum of the acceptor and therefore varies the degree of the spectral overlap between the acceptor and the donor. This subsequently affects the FRET between the donor and the acceptor. In our method, the lifetime of the donor fluorophore is dependent on the FRET and measured using phase-modulation fluorometry. Therefore, the phase angle change which is a function of the lifetime of the donor can be used as a parameter of measuring NH_3 concentration.

MATERIALS AND METHODS

Materials

The ethyl cellulose (ethoxyl content 46%) (EC), tributyl phosphate (TBP), bromocresol green (BCG), and sulforhodamine 101 (SR101) were purchased from Aldrich or Sigma and used without further purification. Gases, i.e., pure nitrogen and nitrogen-balanced ammonia at a concentration of 0.1% (or 1000 ppm–parts of NH_3 per million parts of the total volume), were from Potomac Airgas (Linthicum, MD). Gas mixtures with NH_3 levels less than 0.1% were obtained by blending pure nitrogen with the 0.1% NH_3 through two flow-meter tubes (Series 150, Advanced Specialty Gas Equipment Corp., South Plainfield, NJ).

[2]Abbreviations used: FRET, fluorescence resonance energy transfer; EC, ethyl cellulose; TBP, tributyl phosphate; BCG, bromocresol green; SR101, sulforhodamine 101; RH, relative humidity; LED, light-emitting diode.

Sensor Preparation

The preparation of the sensor film was adapted from Mills *et al.* (25–28). A solution was prepared by dissolving 10 g of EC in a solvent mixture of 20 ml ethanol and 80 ml toluene. Then 1 g of the EC solution was mixed with 0.15 ml of TBP, 0.15 ml of 8.5 mM BCG in methanol, and 0.015 ml of 6.2 mM SR101 in methanol. After the solution was sufficiently mixed, a wet film of uniform thickness was created by placing the solution on a microscope slide with a thickness of 1 mm and drawing the slide under a razor blade clamped approximately 240 μm above the slide. The film was allowed to dry in the air for half an hour before use. The thickness of the dried film was measured using a micrometer which has a resolution of 25.4 μm (or 0.001 in.). As the resolution of the micrometer is not high, the thickness of the dried film was also estimated from the wet film thickness by a reducing factor of 5 (24–28). An average thickness was then derived as 40 mm.

Measurements

Absorption spectra were measured using a Hewlett–Packard 8452A uv/vis diode array spectrophotometer (Palo Alto, CA). Fluorescence spectra and lifetime mea surements were carried out using an ISS K2 multifrequency phase and modulation fluorometer (Champaign, IL). The light source was an argon ion laser (5000 series, ILT, Utah) operated at the 488-nm line. The scattered light from the sample film and the sup porting microscope glass slide was much stronger than that from a sample solution, especially when the sample film was oriented 45° relative to the incident light beam. To reduce the scattered light, the sample glass slide was placed in a 1-cm glass cuvette, with an angle of almost 90° to the incident beam. The fluorescence was then collected from the edge of the sample glass slide (26). In the lifetime measurements, the scattered light caused a shorter apparent lifetime. This was eliminated by placing an Andover 600FH90 long-wave-pass filter (Salem, NH) in the emission path, which cuts off all the light below 600 nm to ensure no scattered light interference. The reference used in the lifetime measurements was a 0.5% solution of Du Pont Ludox HS-30 colloidal silica in water, which has a lifetime of 0 ns, and its scattering intensity was adjusted by adding proper neutral density filters in its emission path. Gas was delivered to the cuvette containing the sensor using a setup similar to that described in Refs. (25, 26), except that an outlet tube and a cover cap were also used to form a closed gas delivery system. All the measurements were performed at ambient temperature.

RESULTS AND DISCUSSION

The absorption and emission spectra of SR101 in EC/TBP polymer film are shown in Fig. 1 as solid lines. Interestingly, the emission maximum of SR101 in the EC/TBP film is blue-shifted about 20 nm, compared to the emission spectrum of SR101 in an aqueous solution (29) and in an EC/TBP polymer incorporating quaternary ammonium hydroxide as a phase transfer agent (24). This is possibly caused by two factors. Since the polymer matrix retained the indicator dye, BCG (pH range 3.8–5.4, pK_a 4.6 (16)), just about in its protonated form (yellow color), the acid–base environment this polymer matrix provided must be around pH 4 equivalent, while the polymer matrix used in Ref. (24) is under strong alkaline conditions. Another factor which may cause the shift is that this matrix is almost water-free. In contrast, the emission spectrum reported in Ref. (29) was measured in a water solution, and the

polymer matrix used in Ref. (24) was associated with a phase transfer agent which provided a water environment, since the phase transfer agent is often solvated with some water molecules (30). The absorption spectra of protonated and deprotonated BCG in EC/TBP film are also included in Fig. 1 as dotted lines. It can be seen that the absorption spectrum of the deprotonated form of BCG overlaps well with the emission spectrum of SR101.

Further experiments were conducted using the sensor film composed of SR101, BCG, EC, and TBP. First, the emission spectra of the sensor film were measured at different levels of NH_3, and the results are shown in Fig. 2. As expected, the fluorescence intensity de creased with increasing NH_3 concentration. The emission spectra measurements were carried out under conditions similar to those used in the lifetime measurements, i.e., the same light source and the same long-wave-pass filter (Andover 600FH90) in the emission path. Note that the scattered excitation light at 488 nm has been removed. BCG itself has little fluorescence compared to the fluorescence intensity of the SR101 at the NH_3 concentrations of interest (i.e., 2–200 ppm). The shape of the spectra in Fig. 2 appeared to change as the NH_3 concentration increased; i.e., the lower spectra seemed to be broader. It was noted earlier in a preliminary experiment that both pH and NH_3 could alter the shape and intensity of the emission spectra of SR101 alone in EC/TBP film, but not the lifetime of the fluorophore. This may be due to the de protonation of the sulfonic acid group on the SR101 in the basic environment. Since we measure the lifetime, slight changes in intensity and spectral shape will not affect our results. In any case, these variations will be accounted for in the calibration curves.

The lifetime response of the sensor to different levels of NH_3 was determined next by measuring the phase angle and modulation change as a function of frequency at various levels of NH_3. The results are presented in Fig. 3 as solid lines. It is seen that when the concentration of NH_3 increased from 0 to 175 ppm, the phase angles decreased about 25, 31, and 35° at frequencies of 50, 100, and 148 MHz, respectively. Additionally, modulation increased about 11, 18, and 22%. In another experiment, measurements of a SR101-alone film showed no difference between the phase angle vs frequency curves obtained in pure N_2 and 0.1% NH_3, indicating that SR101 itself does not respond to NH_3 at these concentrations. As an illustration, the curve of the SR101 alone in N_2 is given in Fig. 3 as a dashed line. The slight difference between the curves for the donor-only film in N_2 and the donor-plus-acceptor film in N_2 is due to the minor overlap of the absorption spectrum of the acceptor in its protonated form with the emission spectrum of SR101 (see Fig. 1).

Figure 4 shows the nonlinear calibration curves of the phase angle, φ, vs NH_3 levels, P_{NH3}. These data were extracted from curves of phase angle vs frequency (some of which are presented in Fig. 3) at frequencies of 50, 100, and 148 MHz. In practice, it is highly desirable to have linear calibration lines instead of calibration curves because of the considerations of facilitation of calibration and accuracy of measurement. Therefore, an attempt to linearize the curves was made using the ratio of tan (φ_0) (phase angle in N_2) to tan (φ) (phase angle at a specific NH_3 level) instead of the phase angle itself. The ratios obtained in this way form reasonably straight lines when plotted against the levels of NH_3, as illustrated in Fig. 5. The slopes of the straight lines represent the frequency-dependent

sensitivity. In this case, it increases with an increase of the frequency of the modulated light in the measured frequency region.

The time response and recovery of the sensor to NH_3 in dry N_2 are demonstrated in Fig. 6, solid line. At a typical film thickness of 40 μm, when the gases sup plied were switched between N_2 and 171 ppm NH_3, the response and recovery times of 90% of the total phase angle change are about 1 and 2.5 min, respectively. The response and recovery times may be shortened by casting a thinner film and/or increasing the plasticizer content, to the extent that the response and recovery processes are diffusion controlled (31,32).

The interference of O_2, CO_2, and humidity with the sensor was studied. Tests of 20% O_2 or 6% CO_2 indicated no interference of these species with the sensor response. However, when humid N_2 was used instead of dry N_2, the phase angle decreased about 5°. This is illustrated in Fig. 6 as a dotted line. The humid N_2 was obtained by allowing the dry N_2 to bubble through a container of distilled water which provided a relative humidity (RH) of 100%. This phase angle shift may only occur for the completely dehydrated state of the sensor, because in a separate experiment in which a NaCl-saturated solution (RH 30.5% (33)) was used instead of pure distilled water, the same phase angle shift was found. As the sensor is essentially based on pH change, acidic or alkaline vapor may interfere with the sensor if it has a proper pK_a to drive pH changing in the range of 3.8 to 5.4–the range in which BCG is sensitive. To verify reproducibility of the measurement, the phase angles of three freshly prepared sample films were measured. Identical phase angle values (i.e., 60.5, 60.3, and 60.7° at 100 MHz in N_2) were obtained over a series of measurements, indicating that the reproducibility of the measurements was very good. Sensor-to-sensor variation could be improved with increased accuracy in film preparation. To demonstrate the long-term stability of the film sensor, the phase angle of a sample film was measured at 100 MHz in both N_2 and 161 ppm NH_3 every day for a period of 5 days, during which no special care of the film was taken. The results shown in Fig. 7 indicate that the phase angles in N_2 remained very constant, while those in 161 ppm NH_3 gradually decreased. This may be due to a slow change of the acid–base environment of the polymer matrix.

We have previously demonstrated a low-cost, optical oxygen sensor (34). By using a blue LED as light source and monitoring the phase angle change at a single frequency (for example, at 25 MHz where the LED can be modulated fairly well), it is possible to build a low-cost instrumentation package for the lifetime-based, optical NH_3 sensor. A discussion on how to build an inexpensive detection system for a lifetime-based sensor measuring in frequency domain has been given in Ref. (35), which may be referred to by interested readers. In addition, by covering the sensor with a thin silicone layer, it should be possible to monitor the dissolved NH_3 in a liquid phase such as in a bioreactor.

CONCLUSION

A lifetime-based FRET NH_3 sensor has been developed for gas-phase NH_3 monitoring. This sensor is not sensitive to the variation in light source intensity or leaching and photobleaching of the indicator dyes. The sensor is useful in an NH_3 range of 2 to 200 ppm. The calibration of the sensor's response to different levels of NH_3 can be linearized by

proper treatment of the data acquired. For a film thickness of 40 μm, the sensor shows response and recovery times for 90% of the total phase angle change of 1 and 2.5 min, respectively. Twenty percent O_2 or 6% CO_2 does not interfere with the sensor, although humidity does. The phase angle measurements for the same sample are reproducible for 5 days, without any special care of the film sample.

ACKNOWLEDGMENTS

The authors gratefully acknowledge the financial support for this research from the National Science Foundation (Grants BES-9413262 and BCS-9157852), the National Institute of Health (Grants RR-08119 and RR-07510), and Genentech, Inc. Q. Chang also thanks Ms. Lisa Randers-Eichhorn for her patient reading of the manuscript and for making grammatical corrections.

REFERENCES

1. Wolfbeis OS (Ed.) (1991) Fiber Optic Chemical Sensors and Biosensors, Vol. I and II, CRC Press, Boca Raton, FL.
2. Lakowicz JR (Ed.) (1994) Topics in Fluorescence Spectroscopy, Vol. 4, Probe Design and Chemical Sensing, Plenum Press, New York.
3. Seitz WR (1988) CRC Crit. Rev. Anal. Chem 19, 135–173.
4. Rao G, Bambot SB, Kwong CW, Szmacinski H, Sipior J, Holavanahali R, and Carter G (1994) *in* Topics in Fluorescence Spectroscopy, Vol. 4, Probe Design and Chemical Sensing (La kowicz JR, Ed.), pp. 417–448, Plenum Press, New York.
5. Uttamlal M, and Walt DR (1995) Biotechnology, 13, 597–601.
6. Lakowicz JR (1983) Principles of Fluorescence Spectroscopy, Plenum Press, New York.
7. Lippitsch ME, and Draxler S (1993) Sens. Actuators B, 11, 97–101.
8. Charlesworth JM, and McDonald CA (1992) Sens. Actuators B, 8, 137–142.
9. Reichert J, Sellien W, and Ache HJ (1991) Fresenius' J. Anal. Chem 339, 467.
10. Reichert J, Sellien W, and Ache HJ (1991) Sens. Actuators A, 25–27, 481–482.
11. Shahriari MR, Zhou Q, and Sigel GH Jr. (1988) Opt. Lett 13, 407–409. [PubMed: 19745914]
12. Zhou Q, Kritz D, Bonnell L, and Sigel GH Jr. (1989) Appl. Opt 28, 2022–2025. [PubMed: 20555459]
13. Giuliani JF, Wohltjen H, and Jarvis NL (1983) Opt. Lett 8, 54–56. [PubMed: 19714133]
14. Kar S, and Arnold MA (1992) Anal. Chem 64, 2438–2443. [PubMed: 1361308]
15. Wolfbeis OS, and Posch HE (1986) Anal. Chim. Acta 185, 321–327.
16. Sellien W, Czolk R, Reichert J, and Ache HJ (1992) Anal. Chim. Acta 269, 83–88.
17. Klein R, and Voges E, (1993) SPIE, Vol. 1885, Advances in Fluorescence Sensing Technology, pp. 81–92.
18. Rhines TD, and Arnold MA (1988) Anal. Chem 60, 76–81. [PubMed: 3344971]
19. Caglar P, and Narayanaswamy R (1987) Analyst (London) 112, 1285–1288.
20. Arnold MA, and Ostler TJ (1986) Anal. Chem 58, 1137–1140.
21. Modlin AN, and Milanovich FP (1991) in Fiber Optic Chemi cal Sensors and Biosensors (Wolfbeis OS, Ed.), Vol. I, pp. 244–245, CRC Press, Boca Raton, FL.
22. Weigl BH, and Wolfbeis OS (1995) Anal. Chim. Acta 302, 249–254.
23. Lakowicz JR, Szmacinski H, and Karakelle M (1993) Anal. Chim. Acta 272, 179–186.
24. Sipior J, Bambot S, Romauld M, Carter GM, Lakowicz JR, and Rao G (1995) Anal. Biochem 227, 309–318. [PubMed: 7573952]
25. Mills A, Chang Q, and McMurray N (1992) Anal. Chem 64, 1383–1389.
26. Mills A, and Chang Q (1993) Analyst (London) 118, 839–843.
27. Mills A, and Chang Q (1994) Sens. Actuators B 21, 83–89.
28. Mills A, and Chang Q (1994) Anal. Chim. Acta 285, 113–123.

29. Haugland RP(1992–1994) Handbook of Fluorescent Probes and Research Chemicals, 5th ed., p. 166, Molecular Probes, Inc.
30. Dehmlow EV, and Dehmlow SS (1980) Monographs in Mod ern Chemistry: Phase Transfer Catalysis, Chap 1, Verlag Chemie, Weinheim.
31. Chang Q, and Mills A Unpublished data.
32. Mills A, and Chang Q (1992) Analyst (London), 177, 1461–1466.
33. Weast RC, Astle MJ, and Beyer WH (Eds.) (1983) CRC Handbook of Chemistry and Physics, 64th ed., p. E–42, CRC Press, Boca Raton, FL.
34. Bambot SB, Holavanahali R, Lakowicz JR, Carter GM, and Rao G (1994) Biotechnol. Bioeng 43, 1139–1145. [PubMed: 18615527]
35. Sipior J, Randers-Eichhorn L, Lakowicz JR, Carter GM, and Rao G Submitted.

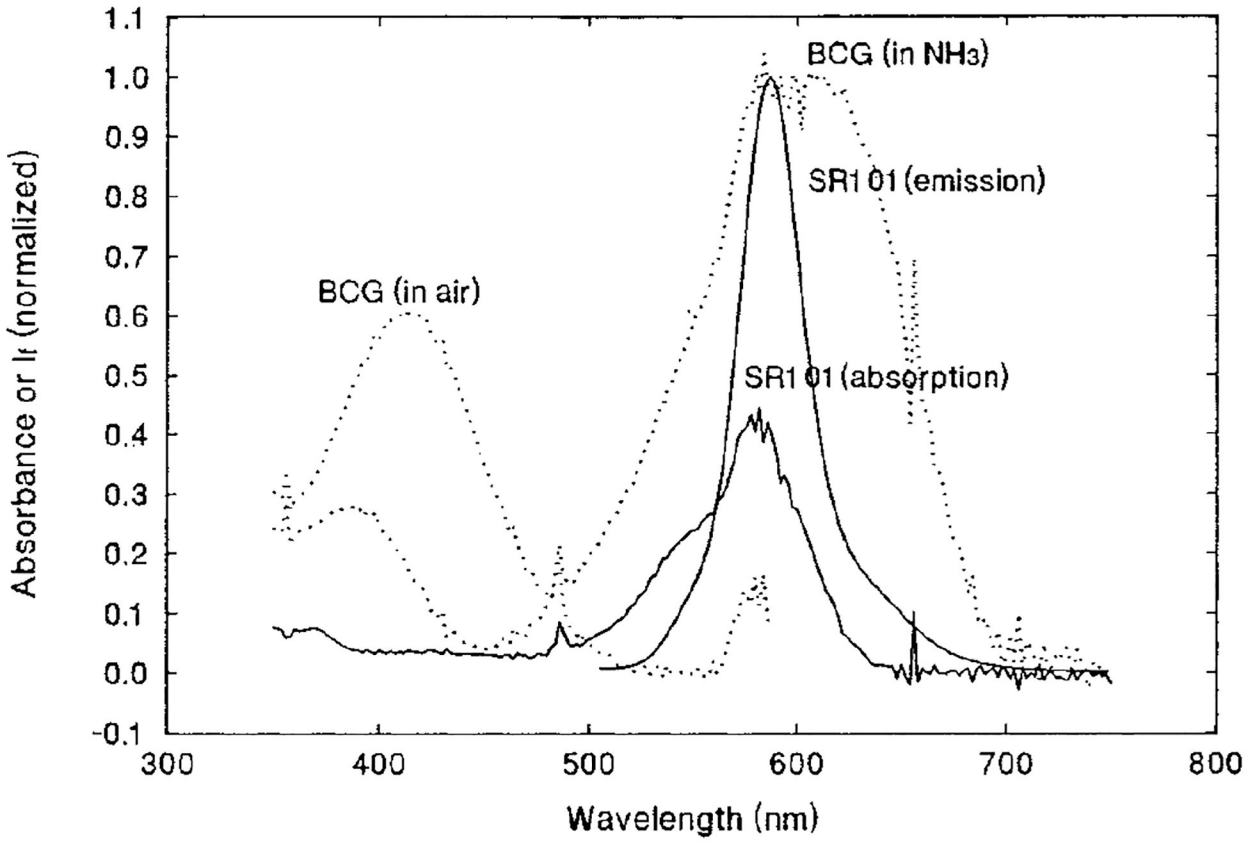

FIG. 1.

Normalized absorption and emission spectra of SR101 in EC/TBP film (solid lines); the dotted lines represent the absorption spectra of BCG in EC/TBP film in NH_3 and in air.

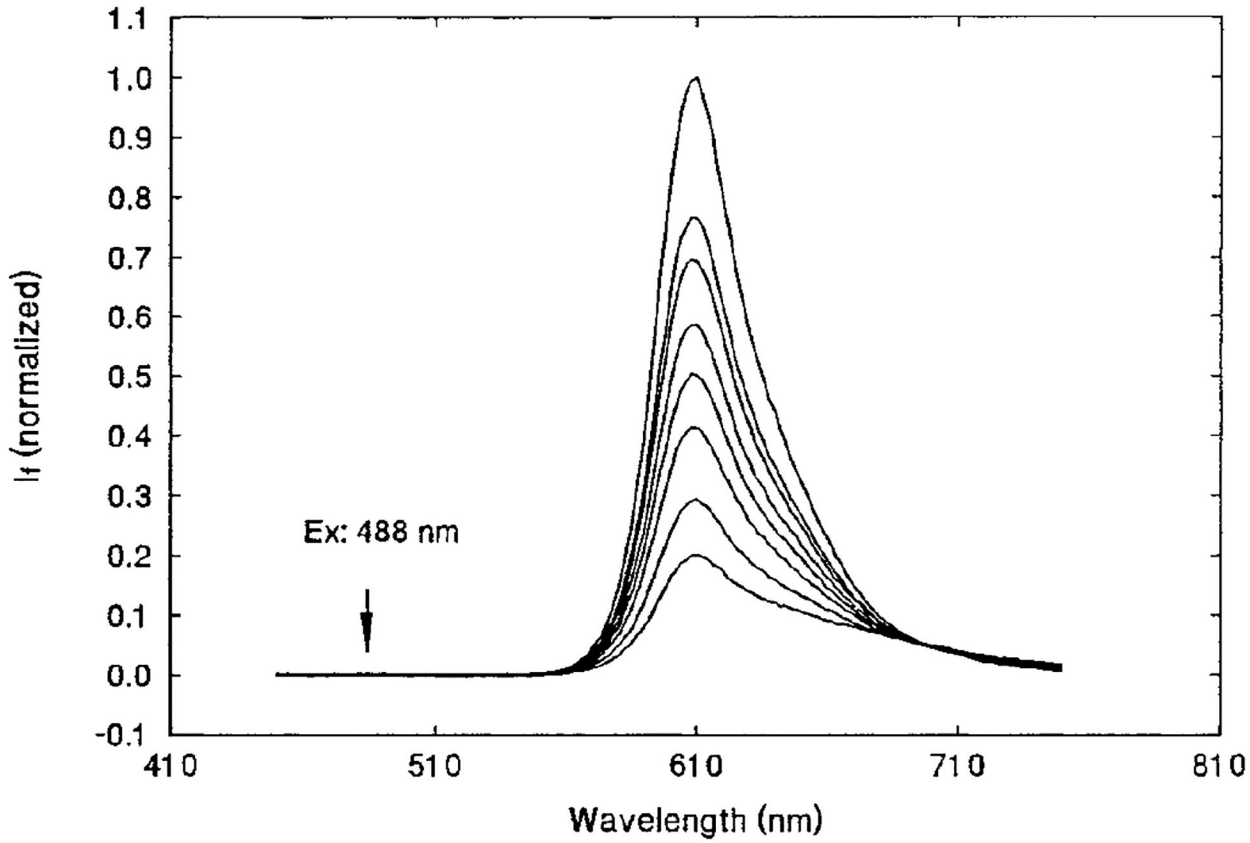

FIG. 2.

SR101/BCG/EC/TBP film sensor in 0, 6.83, 15.1, 30.8, 43.9, 61.0, 110, and 175 ppm NH_3 (from top to bottom). Excitation wave length of 488 nm is indicated by the arrow. Emission was measured with an Andover 600FH90 long-wave-pass filter.

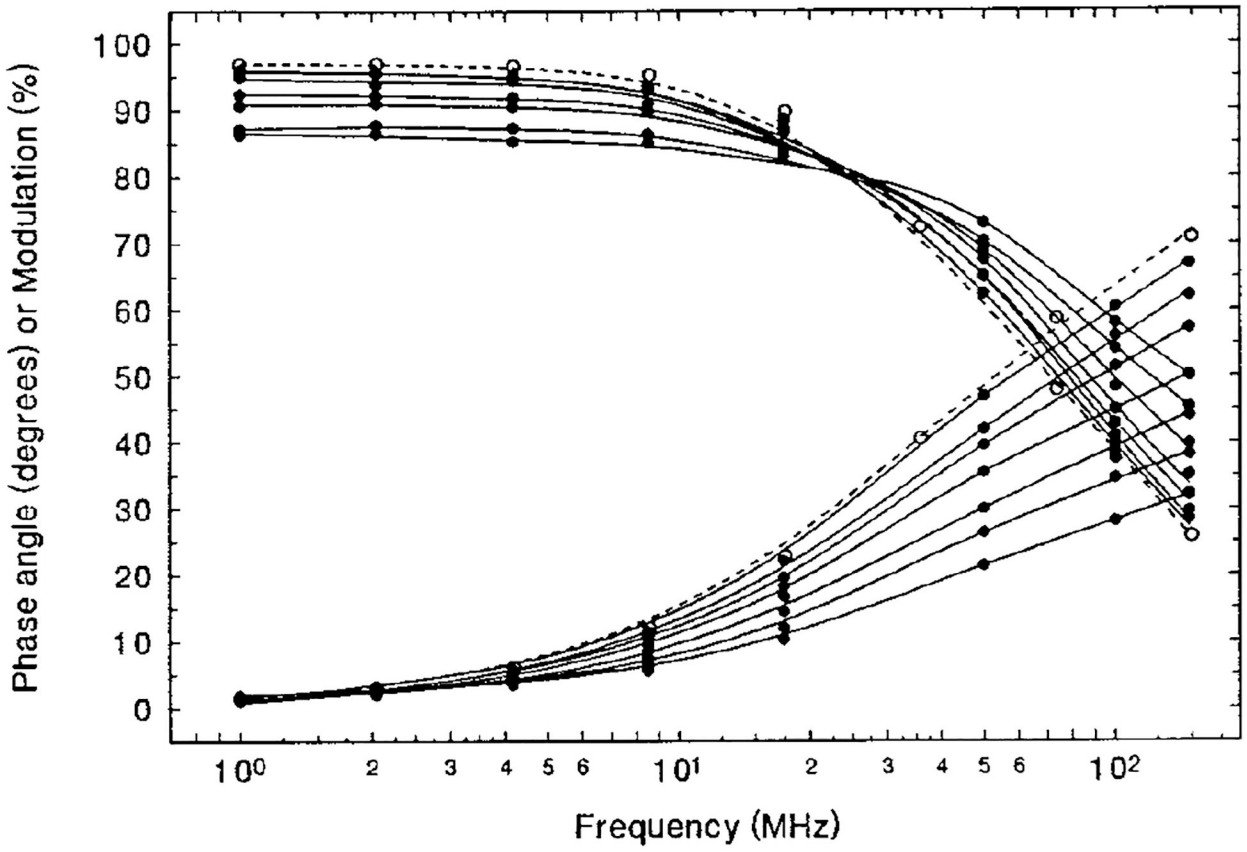

FIG. 3.

SR101/BCG/EC/TBP film sensor (solid lines) in 175, 135, 87.5, 52.3, 30.8, 10.5, and 0 ppm NH_3 (from bottom). SR101 alone in EC/TBP film is shown with dashed lines. Excitation is at 488 nm, with emission collected through an Andover 600FH90 long-wave-pass filter.

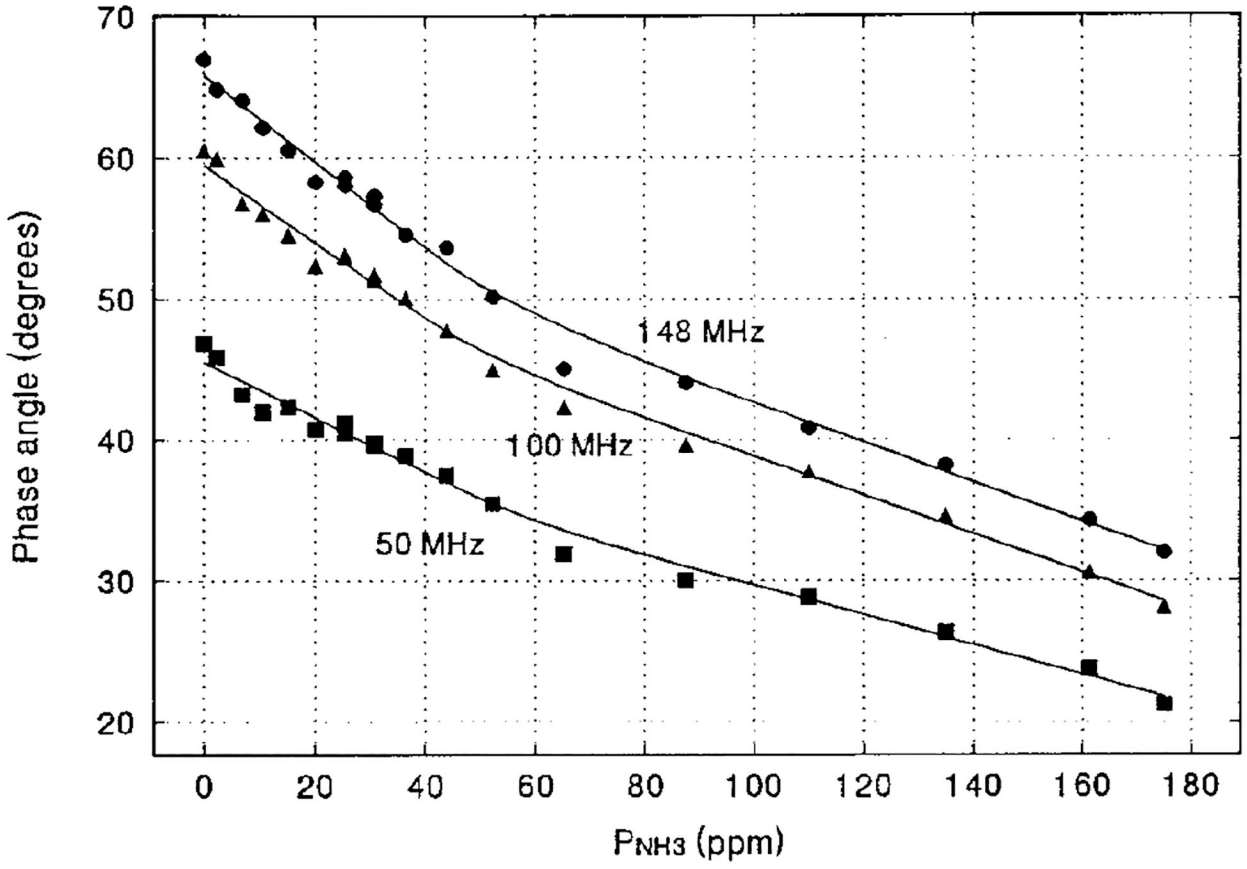

FIG. 4.

Calibration curves of phase angle, φ, versus P_{NH3} for SR101/BCG/EC/TBP film sensor. Excitation is at 488 nm, with emission collected through an Andover 600FH90 long-wave-pass filter.

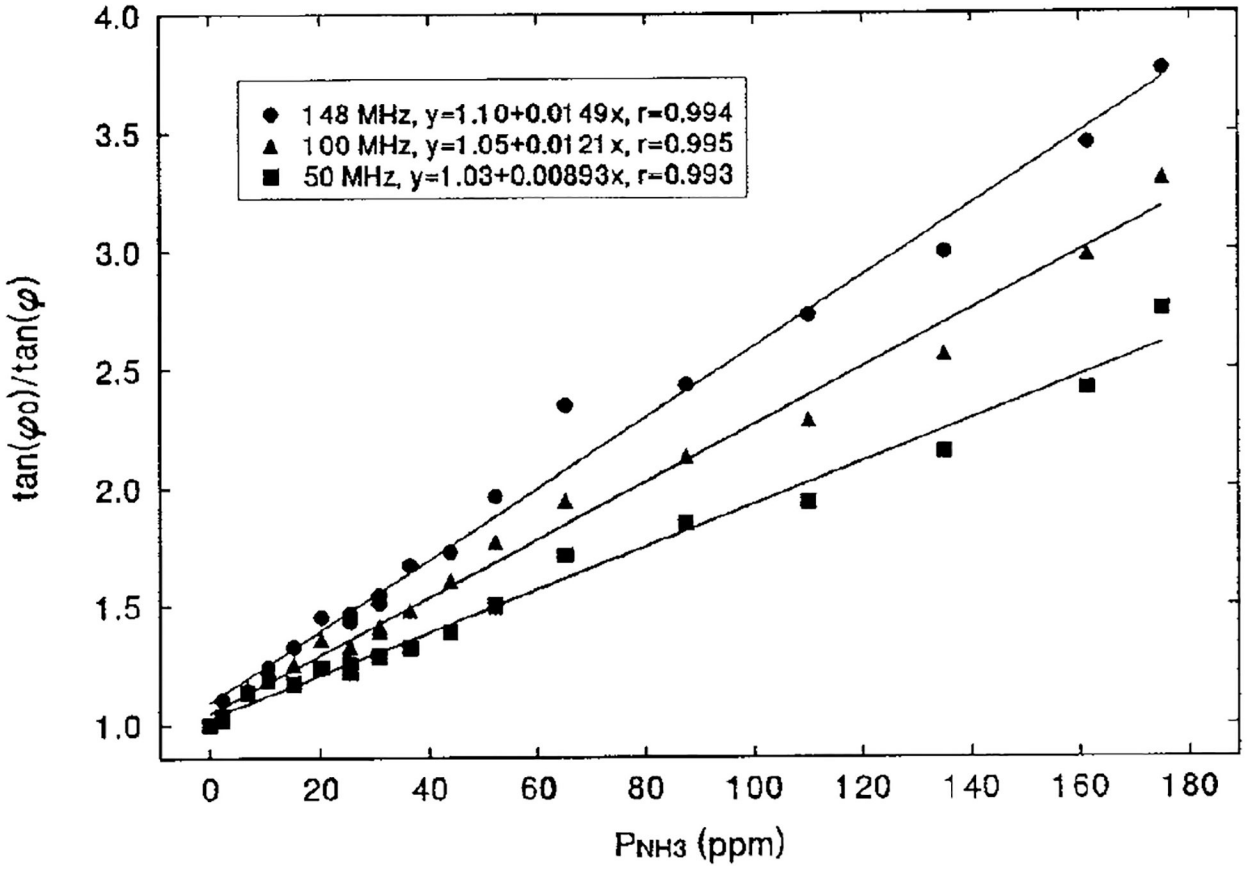

FIG. 5.

Calibration lines of tan (φ_0)/tan (φ) versus P_{NH3} for SR101/BCG/EC/TBP film sensor. Data derived from Fig. 4.

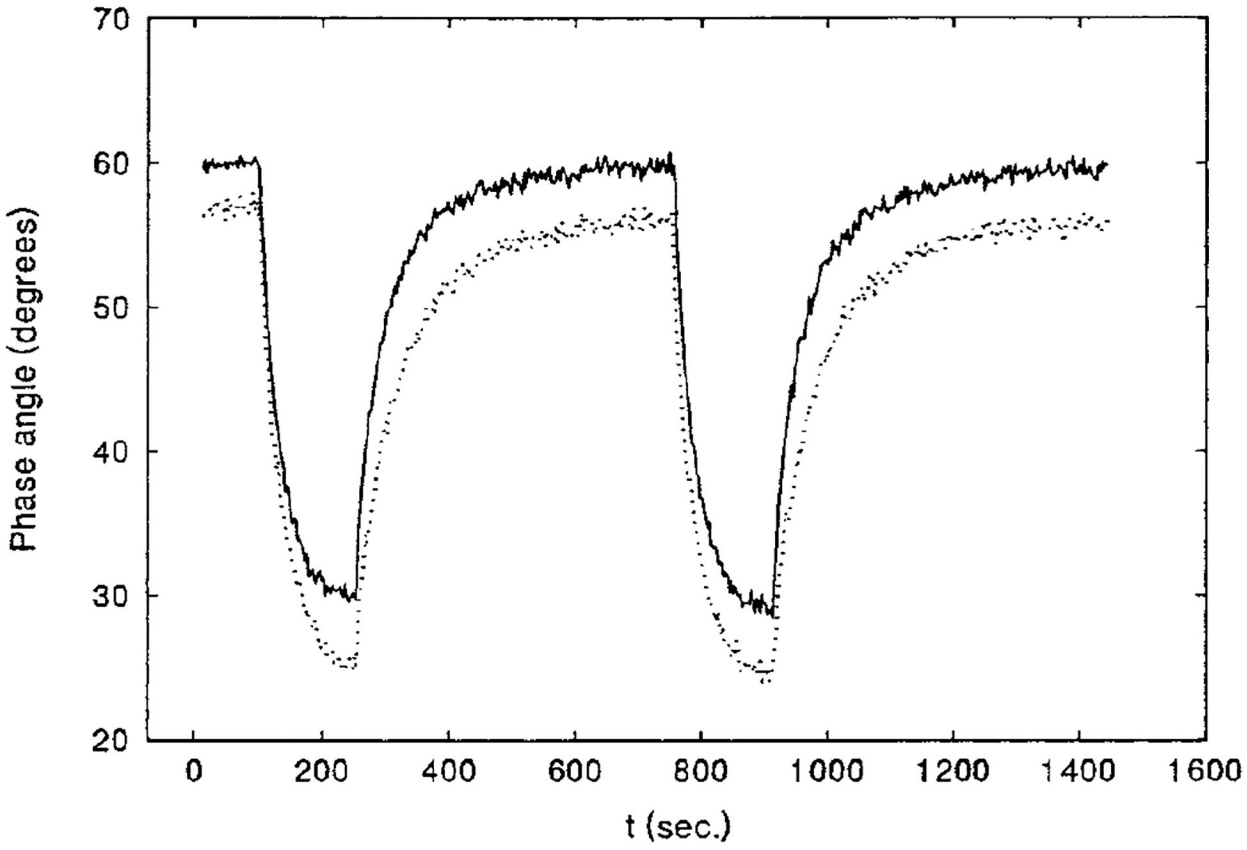

FIG. 6.

Time-dependent response and recovery of SR101/BCG/EC/TBP film sensor in an alternating gas supply of pure N_2 and 171 ppm NH_3 balanced with N_2. Solid line, dry N_2; dotted line, humid N_2. Ex, 488 nm; em, 600FH90 filter; frequency, 100 MHz.

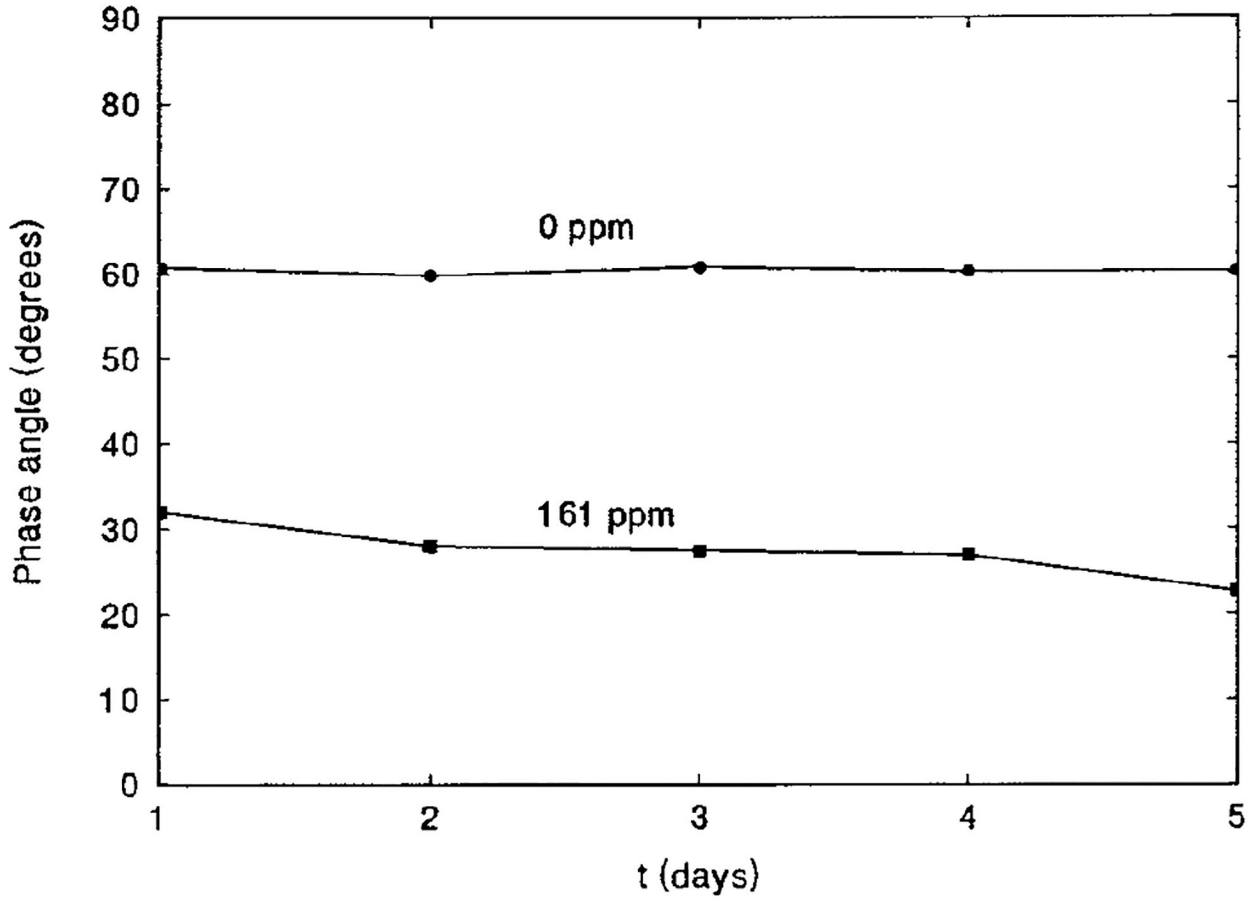

FIG. 7.

Long-term stability of SR101/BCG/EC/TBP film sensor in N_2 and in 161 ppm NH_3. Ex, 488 nm; em. 600FH90 filter; frequency,: 100 MHz.